Compact stand-alone atomic force microscope

Kees. O. van der Werf, Constant A. J. Putman, Bart G. de Grooth, Frans B. Segerink, Eric H. Schipper, Niek F. van Hulst, and Jan Greve
Department of Applied Physics, University of Twente, P.O. Box 217, 7500 AE Enschede, The Netherlands

(Received 14 June 1993; accepted for publication 24 June 1993)

A stand-alone atomic force microscope (AFM) featuring large scan, friction measurement, atomic resolution, and liquid operation, has been developed. Cantilever displacements are measured using the optical beam deflection method. The laser diode and focusing lens are positioned inside the piezo tube and the cantilever at the end of the piezo tube. Because the laser beam stays on the cantilever during scanning, the scan range is solely determined by the characteristics of the piezo tube. In our case $30\times30\times9.5$ μm^3 (xyz). The optical beam deflection detection method allows simultaneous measurement of height displacements and torsion (induced by lateral forces) of the cantilever. AFM images of dried lymphocytes reveal features in the torsion images, which are only faintly visible in the normal height images. A new way of detecting the nonlinear behavior of the piezo tube is described. With this information the piezo scan is linearized. The nonlinearity in a 30-μm scan is reduced from 40% to about 1%, as is illustrated with images of a compact disk. The stand-alone AFM can be combined with a (confocal) inverted microscope, yielding a versatile setup for biological applications.

I. INTRODUCTION

In the standard design of an atomic force microscope (AFM) the cantilever with tip is at rest and the sample is scanned with a piezo-electric xyz translator. The major advantage of this design is the relatively simple mechanical construction of the tip displacement detection. In the case of the optical beam deflection method[1] this consists of a frame containing a laser diode, an adjustable mirror to manipulate the reflected beam and a segmented photodiode. An alternative approach is that the tip is scanned and the sample is at rest. This enables one to image samples of any kind and size. Such a layout is usually called a stand-alone AFM. The microscope head incorporates the force sensor, the scanner and the detection system. Several types of stand-alone AFMs have been built,[2–5] but they all have their specific drawbacks. The setups by Hipp *et al.*,[2] Putman *et al.*,[3] and Baselt *et al.*[5] use optical beam deflection for displacement detection. The laser beam is fixed and the tip scans through the waist of the laser. It is clear that the scan range is limited [5 μm (Refs. 2 and 3) and 1.8 μm (Ref. 5)], due to the limited dimensions of the cantilever and the laser beam waist. The layout of Sarid *et al.*[4] uses optical feedback into the cavity of the diode laser for displacement detection.[6] Since the laser diode and the cantilever are scanned simultaneously, the scan range of this AFM is only limited by the characteristics of the piezo tube used. This AFM, however, cannot be operated under liquid. A major advantage of the optical beam deflection based systems over the design using optical feedback into the laser, is the fact that height displacements and torsion of the cantilever, induced by lateral forces (e.g., friction forces), can be monitored simultaneously in real time.[7]

At the moment several types of stand-alone AFMs are commercially available. The design by Sarid *et al.* is available from Digital Instruments[8] and Topometrix has a stand-alone AFM based on optical beam deflection.[9] The latter design incorporates piezo stacks for large scans, which translate cantilever and laser diode simultaneously. For small scans (<3 μm) a piezo tube is used (similar to the layouts of Hipp *et al.*,[2] Putman *et al.*,[3] and Baselt *et al.*[5] the cantilever is then scanned within the waist of the laser beam).

In this paper we present a stand-alone AFM combining the positive features of the designs mentioned above. The key element in the design is the fact that the laser diode (positioned inside the piezo tube) and the cantilever (at the end of the piezo tube) are scanned simultaneously. Therefore the scan range is only limited by the characteristics of the piezo tube. Furthermore, information on height and lateral forces can be acquired simultaneously and liquid operation is also possible. Inherent in the layout is a new way of detecting the nonlinear behavior of the piezo tube. This information is used to linearize the scan. It is demonstrated that the stand-alone AFM can be used as an add-on unit on the sample stage of a high-resolution inverted optical microscope (NA of 1.3). This configuration is ideally suited for biological applications.

II. DESIGN OF THE STAND-ALONE AFM

A. Layout of the microscope head

The stimulus to design a new AFM came from the fact that the existing AFM in our laboratory[10] did not meet our increased demands. The performance of the integrated inverted optical microscope was not adequate; the numerical aperture (NA) of the lens (taken from a compact disk player, Philips, Netherlands) used was only 0.40. A high level of chromatic aberration limited the use of this optical microscope to monochromatic reflection microscopy (on dried samples) only. Other light microscopic techniques, such as fluorescence, phase contrast, dark field, etc., could not be performed. In our opinion there were two ways to solve this problem: (1) redesign the existing AFM and integrate a better optical system, or (2) design an AFM

 0034-6748/93/64(10)/2892/6/$6.00

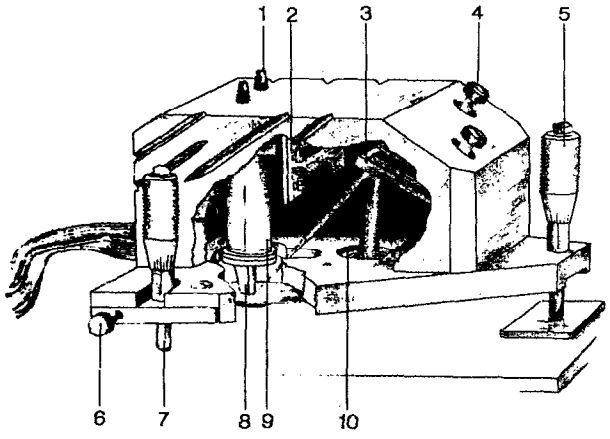

(a)

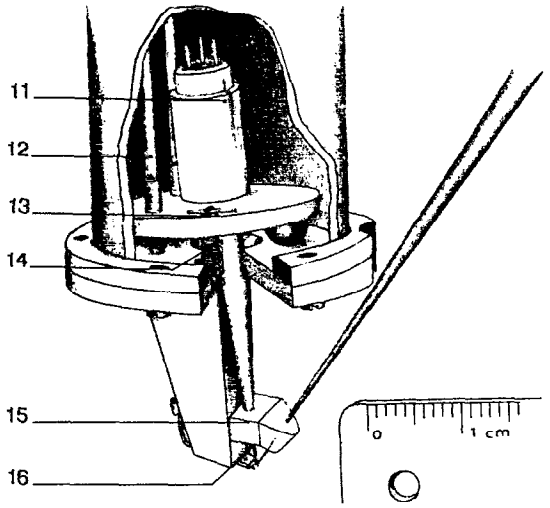

(b)

(c)

FIG. 1. The stand-alone atomic force microscope. (a) Overall layout: (1) adjustment knobs for manipulation of the laser beam, (2) preamplifier electronics, (3) beam-steering mirror, (4) adjustment knobs for the mirror; (5) fine approach; (6) adjustment knobs for cantilever alignment with the optical axis, (7) coarse approach, (8) cantilever holder, (9) piezo tube, (10) quadrant detector. (b) Close-up of essential part: (11) laser diode + focusing lens, (12) flexible rods, (13) adjustable plate, (14) springs, (15) optical window for laser beam, (16) cantilever. (c) Stand-alone AFM combined with an inverted optical microscope.

which can be combined with commercially available optical microscopes. Several arguments (including quality of the optical system, scan range, ease-of-use) were in favor of pursuing the second option and a stand-alone AFM, compatible with any inverted optical microscope, has been developed.

Figure 1(a) shows a systematic representation of the stand-alone AFM. Both cantilever and laser diode are attached at one end of the piezo tube; while scanning, the laser beam stays on the back of the cantilever. A detailed drawing of this part is depicted in Fig. 1(b). The chip with cantilevers with integrated pyramidal tips (Park Scientific Instruments, Sunnyvale, CA) is kept in position by a steel wire. The diode laser (experimental type: 785 nm, 1 mW; Philips, Netherlands) and focusing lens (from a compact disk player: diameter 8.5 mm, focal length 4.5 mm; Philips, Netherlands) are located on an adjustable plate. This plate is firmly coupled to the cantilever holder by two strong springs. By turning the adjustment knobs [see Fig. 1(a)], coupled by flexible PVC rods to the screws in the plate [see Fig. 1(b)], the laser beam can be directed at the cantilever. The reflected laser beam goes via an adjustable mirror (mirror mount MM-1, NRC, Fountain Valley, CA) to a quadrant detector (SPOT-9D, UDT, Hawthorne, CA) monitoring the deflection and torsion of the cantilever. A small piece of Plexiglas attached to the cantilever holder, just above the cantilever [Fig. 1(b)], acts as an optical window for the laser beam enabling liquid operation. This Plexiglas piece is designed in such a way that the laser beam transverses the air- (or liquid-) glass interfaces under right angles, minimizing refraction effects of the laser beam. The mechanical assembly holding the components consists of a brass box attached to a base plate. The total assembly rests on a tripod construction formed by two micrometer screws (Mitutoyo, Japan) for coarse approach and one for the (manual) fine approach.

Positioning a laser diode and a focusing lens on an adjustable plate inside a piezo tube demands a piezo tube with a fairly large inner diameter. Piezo tubes with larger diameters, however, have a smaller scan range. On the other hand, making the tube longer will increase the scan range.[11] For our purposes a piezo tube with an inner diameter of 17 mm, a length of 50 mm and a wall thickness of 1 mm (EBL No. 3, Staveley Sensors Inc., Hartford, CT) was the best compromise with respect to the ultimate physical size of the AFM (height $\times$ width $\times$ length: $80\times80\times110$ mm^3) and the scan range (xyz: $30\times30\times9.5$ μm^3 at ±220 V). The calibration of the AFM has been performed on a crossed grating (xy) with latex spheres (z) (Electron Microscopy Sciences, Fort Washington, PA) for large

scans and on mica for atomic resolution scans.

The design of the fluid cell is very similar to the fluid cell used by LEICA (Wetzlar, Germany) for the confocal laser scanning microscope. A cover slip (with sample) constitutes the bottom of an open cup. The cover slip is pushed into a stainless-steel holder by a stainless-steel ring carrying two rubber O-rings sealing the fluid cell. The Plexiglas nose piece [see Fig. 1(b)] goes down into the cup like a diving glass.

B. AFM combined with an inverted optical microscope

As shown in Fig. 1(c), the stand-alone AFM can be combined with an inverted optical microscope (Axiovert 135, Zeiss, Germany). A hinge construction of the coarse-approach screws [see Fig. 1(a)] makes it possible to move the tip in orthogonal directions (using a V groove and a hole for the coarse-approach screws in the sample stage of the optical microscope), enabling one to get the tip in the center of the field-of-view of the optical microscope. The (biological) sample on a microscope slide or on a cover slip (for low level fluorescence microscopy using high numerical aperture objectives or liquid operation) can be translated in between the tip and the microscope objective with a sample holder/manipulator (Edmund Scientific, Barrington, NJ). This sample holder pushes the microscope slide down onto the sample stage, minimizing the mechanical path length between tip and sample. The total combination is positioned on a concrete slab suspended from the ceiling with elastic cords for vibration isolation.

The Zeiss microscope was selected, because the illumination module for transmission microscopy (differential interference contrast, phase contrast, bright field) can be rotated backward very easily to create space for the AFM [see Fig. 1(c)]. Also, the mechanical layout seemed to be more stable when compared to other candidate inverted optical microscopes: the sample stage is supported at three points. The optical image can be observed by eyepieces or by a charge-coupled device (CCD) camera and monitor. It is obvious that during AFM operation only fluorescence (epi-illumination) and reflection microscopy (on dried samples) can be performed.

C. Control electronics and data acquisition

The data acquisition is based on a 50 MHz 486 PC carrying analog-to-digital converter and digital-to-analog converter on board (PCL-818, Advantech Co., Taiwan). The scan software was designed in order to have a maximal flexibility, e.g., open structure. The program is able to capture and display eight signals (four parameters, back and forth scans) simultaneously. The control electronics, such as high-voltage amplifiers, low noise preamplifier electronics in the AFM head [see Fig. 1(a)], scan control module, feedback module, and signal-selection and filter modules, are all home built. Height, deflection, torsion, and external signals may be selected. The height signal displays the voltages applied to the z electrode of the piezo when the feedback loop is closed. Even while the feedback loop is closed, some displacements of the cantilever remain. This signal is displayed when the deflection option (also error signal; Ref. 12) is selected. In short: the height signal gives the low-pass filtered version and the deflection signal the high-pass filtered version of the topography. The bandwidth of this "hardware filter" (crossover point from low- to high-frequency information) is determined by the integration time in the feedback loop and ultimately by the resonance frequency of the piezo tube. The torsion parameter monitors the movement of the cantilever (while scanning the cantilever perpendicular to its long axis) resulting in a shift of the laser spot at the photodiode perpendicular to the deflection direction.[13] This parameter gives information on the friction forces between tip and surface.[14]

III. FORCE CONTROL AND SCAN LINEARIZATION

From Fig. 1(a) it is clear that even during scanning completely free from the surface, the laser spot will move over the detector. As a result a ramp-shaped variation in the deflection signal is observed. Basically, the position of the cantilever in the xy plane is detected. This signal variation generates a pseudotilt in the AFM height image. Of course, this tilt in the image can be easily removed by software. But what is more important is that, when operated in closed loop, the applied force is not constant, because the feedback loop reacts to this pseudotilt. In our layout this artificial tilt is 0.02° for 100-μm and 0.04° for 200-μm cantilevers. The tilt angle depends on the geometrical amplification factor $2L/l$ (with L cantilever-detector separation and l the length of the cantilever). This artificial tilt induces a variation in applied force of 1 nN over a scan range of 30 μm (force constant of 200-μm cantilever: 0.06 N/m). This force variation can be reduced by adding a percentage of the driving voltage of the piezo tube to the deflection signal (at the preamplifier electronics in the AFM head) before it enters the feedback loop. In this case the variation in force is less than 60 pN over a 30-μm range.

A closer look at the variation in the deflection signal reveals that it is not fully ramp shaped but curved (Fig. 2, line 1). Since the position of the cantilever is detected through the deflection signal (scanning out-of-contact), the curvature must reflect the nonlinear behavior of the piezo tube. Fitting the curved line with a third-order polynom, nonlinear driving voltages can be calculated that result in a fully ramp-shaped variation in the deflection signal (Fig. 2, line 2). This would give a linearization of the piezo movement in the x direction (fast scan), but not in the y direction (slow scan). Time-dependent hysteresis behavior of the piezo rules out the option using identical nonlinear driving voltages for the fast and slow scan. Since a quadrant detector is used, the movement of the laser beam on the detector in the y direction can be monitored using the torsion signal, while scanning out-of-contact. Thus, a typical calibration experiment proceeds as follows. With the laser beam reflecting off a rigid mirror (the holder of the cantilevers) to reduce noise due to cantilever movements, two dummy images are recorded simultaneously. From the first image (showing the deflection sig-

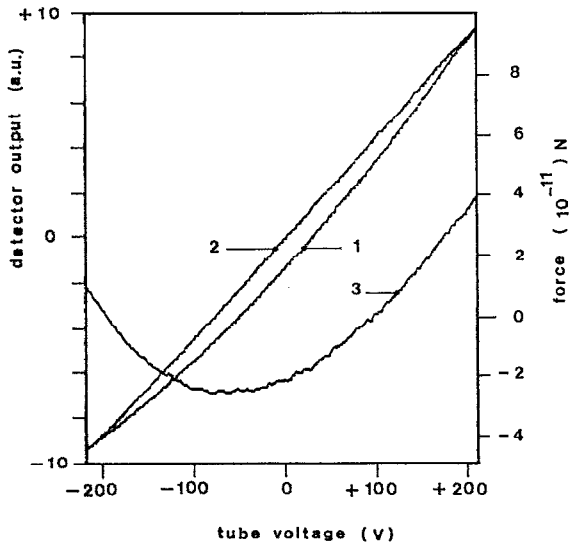

FIG. 2. Laser beam movement on the detector, while scanning out-of-contact. The laser beam reflects off a rigid mirror (the holder of the cantilevers). Line 1: Nonlinear detector output when supplying the piezo tube with a linear driving voltage. Line 2: Linear detector output when supplying the piezo tube with a nonlinear driving voltage. Line 3: Force variation after correction as described in the text. Lines 1 and 2: left axis, line 3: right axis.

nal) a horizontal line is used to calculate the coefficients in the third-order polynom for the fast scan. From the second image (showing the torsion signal) a vertical line is used for the calculation of the coefficients for the slow scan. We define the nonlinearity of the scan as the normalized difference between the maximum and minimum piezo sensitivity within a scan. In a nonlinearized scan this sensitivity varies by 40% over a 30-μm scan range (at 440 V over 1-mm wall thickness of the piezo tube). This reduces to about 1% after linearization, as determined from the coefficients in the polynom.

IV. AFM IMAGING

In Fig. 3 AFM images of the surface of a compact disk (without a polycarbonate coating) are shown. Without linearization a large curvature of the tracks is evident [Fig. 3(a)]. Scanning the same area again, but now supplying the piezo tube with a nonlinear driving voltage, results in a removal of the distortion [Fig. 3(b)]. The residual distortion still faintly visible in Fig. 3(b), is due to the nonflatness of the monitor screen from which pictures are taken with a camera at a distance of 0.5 m.

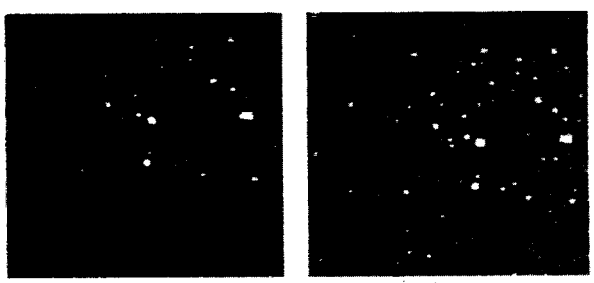

FIG. 3. Effect of scan linearization. AFM images of a compact disk (without the polycarbonate coating) (a) before and (b) after scan linearization. The distance between the tracks is 1.6 μm. Image size: 30×30 μm^2. These images are recorded in open loop (deflection signal).

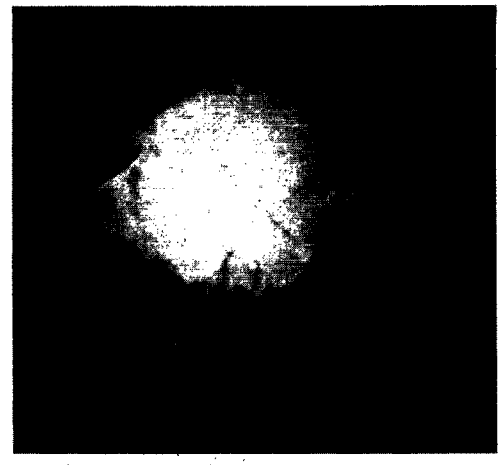

FIG. 4. AFM image of an air dried human lymphocyte. Image size: 30×30 μm^2. This image is recorded in closed loop and the feedback signal supplied to the piezo tube is shown.

As shown in Fig. 1(c), the stand-alone AFM can be combined with an inverted optical microscope. In Fig. 4 and AFM image of an air dried human lymphocyte, which was selected with the optical microscope, is shown. At the bottom side of the cell several pseudopodia are visible. Zooming in on these pseudopodia reveals interesting structures if the torsion signal is monitored also. In Figs. 5(a) and 5(b) the error signal of the back and forth scans is shown: the up slope of objects is white and the down slope is dark. Changing the direction of scanning changes the "shadow" in the image. At the knoblike termination of one of the pseudopodia (left side of the image) the shadow switches from left to right. In Figs. 5(c) and 5(d) the torsion signal of the back and forth scans are shown. Structures are revealed which are not visible in Figs. 5(a) and

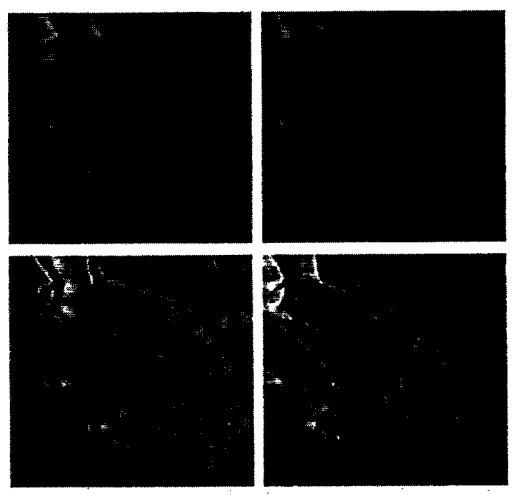

FIG. 5. A detail of pseudopodia at the bottom side of the lymphocyte of Fig. 4. (a,b) Error signal, back and forth scan, (c,d) torsion signal, back and forth scan. Image size: 10×10 μm^2.

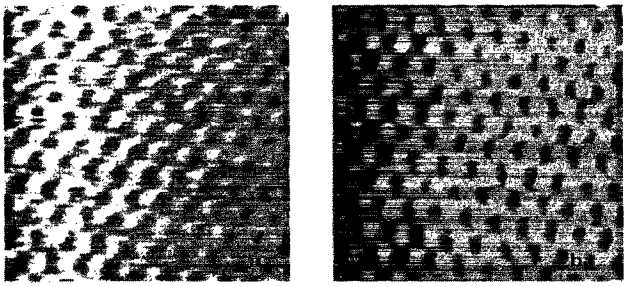

FIG. 6. High-resolution images of mica: (a) height and (b) friction. Image size: 6×6 nm^2.

5(b). Most probably these structures are solubles in the cell medium which are dried. The contrast reversal [comparing Figs. 5(c) and 5(d)] between these structures and the background (glass surface) indicates that the friction coefficient of glass is different from dried solubles. From the high transient torsion signal at the pseudopodia [upper left of Fig. 5(c)] it can be deduced that the friction coefficient of glass is actually higher than the friction coefficient of the dried solubles.

When the AFM is combined with the inverted optical microscope, vibrations with an amplitude of about 2 nm and a frequency around 300 Hz are observed. This is not a limiting factor for most biological applications. On a separate vibration isolated setup (without the optical microscope) it is possible to reduce these vibrations. Replacing the hinges and the Mitutoyo micrometer screws by more rigid micrometer screws (AJS-1, NRC, Fountain Valley, CA), results in a minimal detectable displacement (in contact) in the z direction of 0.1 Å in a bandwidth from 100 Hz to 20 kHz. As is shown in Fig. 6, both in height and friction atomic resolution can be obtained. The hexagonal packing is clearly visible.

V. DISCUSSION

Initial measurements with a prototype stand-alone AFM featuring a stationary laser beam and a scanning tip, indicated that at scan ranges of 20-μm force variations of 100 nN are induced. These variations are due to curvature of the cantilever and variations in the amount of light reflected towards the detector. This large variation in force was the paramount reason to design a stand-alone AFM which scans the light source and the cantilever simultaneously. Line 3 in Fig. 2 shows the residual force variation after correction. Over the maximum scan range of 30 μm this variation is 60 pN, but it decreases quadratically when reducing the scan range. In the setup by Baselt *et al.* (maximum scan range: 1.8 μm) a force variation of 2.6 nN/μm of scan range (spring constant: 0.3 N/m is observed).[5] Due to the limited bandwidth of the feedback loop (being 1800 Hz as determined by the resonance frequency of the piezo tube) transient forces occur during scanning (error signal). These forces can be as high as 10 nN without destroying living glial cells.[15] So a force variation of 60 pN will not be the limiting factor for normal AFM operation. From this it is clear that our system which scans the laser diode and cantilever simultaneously, has two major advantages over systems with a stationary beam: (1) small variations in applied force and (2) large scan area.

Two other methods of piezo linearization in AFM are based on the position detection with light-emitting diodes (LEDs), detectors and fins attached to the piezo: postimaging software image correction and real-time feedback scan correction.[16] An advantage of our method of linearization, preimaging correction, is the fact that no extra opto-electronic components are needed. Furthermore, no feedback loop is used which limits the scan rate and adds noise.[16] A disadvantage stems from the time-dependent behavior of the piezo. If the scan frequency is changed, the calculated coefficients will no longer perfectly match the nonlinear behavior. To minimize this effect, the linearization procedure has been performed at the scan frequencies most frequently used. These calculated coefficients are tabulated and are used at the appropriate scan frequencies.

The current inverted optical microscope has fluorescence and reflection (on dried samples) capabilities while operating the AFM. Because of this, the sample either has to be stained with fluorescent dyes or air dried. A little known optical microscopical technique, reflection contrast microscopy, allows one to obtain reflection images of biological objects under liquid. An oil-immersion objective (NA 1.3), with a quarter-wave plate in front of the objective, gives high-resolution optical images of unstained cells on cover slips. This option will be installed on our inverted microscope within the next few months. In a recent study we have shown that this AFM can also be combined with a confocal laser scanning microscope.[17] In that study the cytoskeleton of stained monkey kidney cells, dried and in physiological buffer, has been imaged quasisimultaneously with this confocal microscope and the AFM. In the future, possibly the stand-alone AFM will be combined with a Raman microscope[18] available in our laboratory.

In agreement with others,[19] we experienced that it is easier to obtain clearer atomic corrugation in the friction images compared to the normal height images. Changing the loading force frequently resulted in large variations in contrast, both in height and in friction. This possibly indicates that at the apex pyramidal tip small protruding nanotips, terminating in single atoms, exist. Changing the loading force changes the interaction site between tip and surface. Furthermore, large differences in contrast between back and forth scans are observed. This again illustrates that the interaction is localized on a subnanometer scale and that the contrast is not due to an averaging effect of contributing interactions between the large pyramidal tip and the surface.[20] Another interesting aspect is that the height and friction signal are out-of-phase. From oscilloscope traces it was observed that the height signal lags the friction signal by about 90°, as was reported before.[7]

A stand-alone atomic force microscope has been presented which features a large scan (xyz: $30 \times 30 \times 9.5$ μm^3), friction measurement, atomic resolution and liquid operation. A new procedure for scan linearization reduces the nonlinearity in the AFM images from 40% to about

1% over a 30-μm scan. The force variations over a 30-μm range are about 60 pN, significantly lower than the force transients (error signal) due to the limited bandwidth of the feedback loop (1800 Hz). The simultaneous measurement of height and torsion signals gives the AFM a sensitivity on the basis of differences in friction coefficients. The stand-alone AFM is combined with an inverted optical microscope, an ideal setup for biological applications.

ACKNOWLEDGMENTS

We thank Klaas Smit, Theo Punt, and Peter Scheeren from the machine shop for machining the mechanical parts. This research was supported by a grant from the Dutch Organization for Scientific Research NWO.

[1] G. Meyer and N. M. Amer, Appl. Phys. Lett. **53**, 2400 (1988).
[2] M. Hipp, H. Bielefeldt, J. Colchero, O. Marti, and J. Mlynek, Ultramicroscopy **42-44**, 1498 (1992).
[3] C. A. J. Putman, H. G. Hansma, H. E. Gaub, and P. K. Hansma, Langmuir **8**, 3014 (1992).
[4] D. S. Sarid, P. Pax, L. Yi, S. Howells, M. Gallagher, and T. Chen, Rev. Sci. Instrum. **63**, 3905 (1992).
[5] D. R. Baselt and J. D. Baldeschwieler, Rev. Sci. Instrum. **64**, 908 (1993).
[6] D. S. Sarid, D. A. Iams, V. Weissenberger, and L. S. Bell, Opt. Lett. **13**, 1057 (1988).
[7] O. Marti, J. Colchero, and J. Mlynek, Nanotechnology **1**, 141 (1990).
[8] Digital Instruments Inc., Santa Barbara, CA.
[9] Topometrix, Santa Clara, CA.
[10] C. A. J. Putman, K. O. Van der Werf, B. G. De Grooth, N. F. Van Hulst, F. B. Segerink, and J. Greve, Rev. Sci. Instrum. **63**, 1914 (1992).
[11] C. J. Chen, Appl. Phys. Lett. **60**, 132 (1992).
[12] C. A. J. Putman, K. O. Van der Werf, B. G. De Grooth, N. F. Van Hulst, J. Greve, and P. K. Hansma, Proc. SPIE **1639**, 198 (1992).
[13] G. Meyer and N. M. Amer, Appl. Phys. Lett. **57**, 2089 (1990).
[14] R. M. Overney, E. Meyer, J. Frommer, D. Brodbeck, R. Lüthi, L. Howald, H.-J. Güntherodt, M. Fujihira, H. Takano, and Y. Gotoh, Nature **359**, 133 (1992).
[15] E. Henderson, P. G. Haydon, and D. S. Sakaguchi, Science **257**, 1944 (1992).
[16] R. C. Barrett and C. F. Quate, Rev. Sci. Instrum. **62**, 1393 (1991).
[17] C. A. J. Putman, A. M. Van Leeuwen, B. G. De Grooth, K. Radosevic, K. O. Van der Werf, N. F. Van Hulst, and J. Greve, BioImaging **1**, 63 (1993).
[18] G. J. Puppels, M. Grond, and J. Greve, Appl. Spectrosc. (to be published).
[19] D. R. Baselt and J. D. Baldeschwieler, J. Vac. Sci. Technol. B **10**, 2316 (1992).
[20] R. W. Tillmann, M. Radmacher, and H. E. Gaub, Appl. Phys. Lett. **60**, 3111 (1992).